A COMPARISON BETWEEN GEOSTROPHIC AND NONGEOSTROPHIC NUMERICAL FORECASTS OF HURRICANE MOVEMENT WITH THE BAROTROPIC STEERING MODEL [1]

By Akira Kasahara

The University of Chicago

(Original manuscript received 13 November 1958; revised manuscript received 13 February 1959)

ABSTRACT

The steering flow of a hurricane is obtained by eliminating the vortex pattern from the total flow field. The evolution of the steering flow is predicted by solving the barotropic nondivergent vorticity equation. Based upon the steering-flow prediction, a forecast of the hurricane movement is obtained with the use of an equation which provides for interaction between the hurricane and the steering flow.

In the geostrophic model, the geostrophic-wind assumption is used in solving the vorticity equation. In the nongeostrophic model, the stream function governed by the 'balance equation' is adopted. With the above two prediction models, 45 pairs of predictions of the 24-hr and 48-hr movement of hurricanes Diane and Connie (August 1955) and Betsy (August 1956) at the 500- and 700-mb levels were prepared by the use of an electronic computer.

A detailed comparison between performances of the two prediction models is presented. Generally speaking, there is a remarkable similarity between the nongeostrophic and geostrophic forecasts of hurricane movement. The accuracy of the 700-mb hurricane forecasts appears to be comparable with that obtained from the 500-mb forecasts. However, for both prediction models, the 'resultant' forecast, which is the vector mean of the 700- and 500-mb predicted displacements, seems to provide a significant improvement over the accuracy of a single-level barotropic forecast. These analyses suggest that further improvements are possible by advancing the prediction model from the barotropic model to the equivalent barotropic or the baroclinic model.

1. Introduction

In a previous article (Kasahara, 1957a),[2] the writer described a numerical method of predicting hurricane movement, and the results of the geostrophic forecasts of hurricanes Diane and Connie (August 1955) at the 500-mb level were presented. Since the prediction model is based upon the assumptions of barotropic and nondivergent motion in the atmosphere, we selected first the 500-mb height as a representative forecasting variable which is suitable for the model. It is conceivable, however, that the levels of nondivergence in a hurricane and in the steering flow may be located at different heights in the atmosphere. Also, the level of nondivergence in a hurricane may change from time to time depending upon the stages of the life cycle and the characteristics of individual hurricanes. There is some evidence that the level of nondivergence in a mature hurricane may be located somewhere between the 500- and 700-mb levels (*e.g.*, Palmén and Riehl, 1957), which agrees more or less with the height of nondivergence in the large-scale flow. Partly for these reasons, hurricane forecasts were prepared using the 700-mb data with the same prediction model, and these forecasts are compared here with those obtained from the 500-mb data.

In order to increase the number of test cases in addition to hurricanes Connie and Diane, we decided to investigate hurricane Betsy, August 1956, for the following reasons. Betsy travelled anticyclonically around the West Atlantic subtropical high; as a consequence, reasonable amounts of upper-air sounding data as well as weather reconnaissance flight data were available to perform the analysis over the hurricane. Although the over-all dimension of Betsy was much smaller than that of Diane, the movement paths were generally alike in these two cases. This seems to provide an ideal case to investigate whether certain types of forecasting errors are related to certain types of steering-flow configurations.

The scheme for computing the steering-flow evolution is based upon the time integration of the barotropic nondivergent vorticity equation. It is, therefore, desirable to employ the stream function instead of using the pressure height as a forecasting variable. By this means, one would also hope to improve the evaluation of the wind field in the tropics where the validity of the geostrophic-wind approximation is questionable and, furthermore, to prevent a spurious

[1] The research reported in this article has been sponsored by the U. S. Weather Bureau, under Contract Number Cwb 9227 with the University of Chicago.

[2] Hereafter, the prediction model described in the article is referred to as the *barotropic steering model*. For further reference, the paper is denoted by BSM.

intensification of the subtropical high which is displayed sometimes in the geostrophic forecasts. Although the stream function has been employed in solving the vorticity equation for the purpose of predicting hurricane movement (Hubert, 1957, and Masuda and Itoo, 1957), no systematic test has yet been made with a view toward examining the differences between geostrophic and nongeostrophic forecasts.

The purpose of this article is to present a comparison between the geostrophic and nongeostrophic forecasts obtained from the same 500- and 700-mb hurricane data and to explore the possibilities for improving the accuracy of hurricane prediction within the framework of the barotropic steering model.

2. Forecasting procedures

Considering the height field z of a constant-pressure surface, the steering flow of a hurricane $\bar{z}$ is defined as the residual flow obtained by eliminating a circular vortex $h(r)$ from the total field z; thus,

$$\bar{z} = z - h(r), \tag{1}$$

where the definition of $h(r)$ is given by

$$h(r) = (1/2\pi)\int_0^{2\pi} z(r, \theta)d\theta - z(\infty) \tag{2}$$

and r, θ are the cylindrical coordinates whose center is taken at the center of a hurricane. The $z(\infty)$ denotes the value of z at the periphery of the vortex. After obtaining the vortex $h(r)$, the $h(r)$ field is subtracted algebraically from the total height z field to get the steering $\bar{z}$ field. Small irregularities left in the steering-flow contours near the vortex center must be smoothed out.

The x and y components of the instantaneous movement velocity of the vortex, $C_{(x)}$ and $C_{(y)}$, are computed from (for the derivation, see BSM)

$$C_{(x)} = \bar{U}_0 - K\bar{\eta}_{y0}, \tag{3a}$$

$$C_{(y)} = \bar{V}_0 + K\bar{\eta}_{x0}, \tag{3b}$$

where $\bar{U}$ and $\bar{V}$ denote the x and y components of the steering velocity and $\bar{\eta}_x$ and $\bar{\eta}_y$ denote the x and y components of the gradient of the steering absolute vorticity, respectively. The subscript zero denotes the value of a quantity evaluated at the vortex center, and K is defined by

$$K = -\lambda(h/\nabla^2 h)_0 = \lambda L^2/4. \tag{4}$$

Here, ∇^2 is the horizontal Laplacian operator, and L is the characteristic scale of the vortex defined as the distance from the center to the position at which the parabola drawn to fit the $h(r)$ profile near the center intersects the $z(\infty)$ line. The factor λ is a constant, the value of which is chosen to be 1.5 (Kasahara, 1957b).

The evolution of the steering velocity components $\bar{U}$ and $\bar{V}$ is determined by solving the barotropic steering vorticity equation

$$\bar{\eta}_t + \bar{U}\bar{\eta}_x + \bar{V}\bar{\eta}_y = 0. \tag{5}$$

Two models are employed here for solving equation (5).

(a) *Geostrophic model.* If one admits the geostrophic-wind assumption, equation (5) may be written in the form

$$\nabla^2\bar{z}_t = J(\bar{\eta}, \bar{z}), \tag{6a}$$

where $J(\alpha, \beta) = \partial(\alpha, \beta)/\partial(x, y)$ for the Jacobian of α and β, and

$$\begin{aligned} \bar{U} &= -f^{-1}g\bar{z}_y, \quad \bar{V} = f^{-1}g\bar{z}_x, \\ \bar{\eta} &= f^{-1}g\nabla^2\bar{z} + f, \end{aligned} \tag{6b}$$

where g and f denote the acceleration of gravity and the Coriolis parameter, respectively. The subscript of a quantity represents a partial derivative.

(b) *Nongeostrophic model.* Since we assume nondivergent motion, the steering stream function $\bar{\Psi}$ may be obtained from the steering height field $\bar{z}$ with the use of the balance equation in the form

$$g\nabla^2\bar{z} = f\nabla^2\bar{\Psi} + 2(\bar{\Psi}_{xx}\bar{\Psi}_{yy} - \bar{\Psi}_{xy}^2) + \nabla f\cdot\nabla\bar{\Psi}, \tag{7}$$

where ∇ denotes the horizontal gradient operator. This equation is derived by applying a horizontal-divergence operator to the primitive equations of steering motion and retaining only the nondivergent part of the wind. Using the stream function $\bar{\Psi}$, equation (5) is expressed by

$$\nabla^2\bar{\Psi}_t = J(\bar{\eta}, \bar{\Psi}) \tag{8a}$$

and

$$\begin{aligned} \bar{U} &= -\bar{\Psi}_y, \quad \bar{V} = \bar{\Psi}_x, \\ \bar{\eta} &= \nabla^2\bar{\Psi} + f. \end{aligned} \tag{8b}$$

For either model, the evolution of the steering flow is determined by solving equation (6a) or (8a); then the displacement of a hurricane center is predicted with the use of the velocity formula (3a, b) together with (6b) or (8b). To obtain the solution of this problem, all computations were performed in finite-difference forms. A lattice network is arranged in a 25×22 array with a square grid of 300 km (shown in fig. 4 of the BSM paper). The time extrapolation is made with one-hour time interval.

As discussed by several authors (*e.g.*, Charney, 1955, and Bolin, 1955), the variational equation of (7) is of elliptic type if $2g\nabla^2\bar{z} + f^2 - 2\nabla f\cdot\nabla\bar{\Psi}$ is positive and there exist two possible solutions, one of which yields a negative absolute vorticity everywhere ($\eta < 0$) and the other a positive absolute vorticity everywhere ($\eta > 0$) in the domain. It is known also

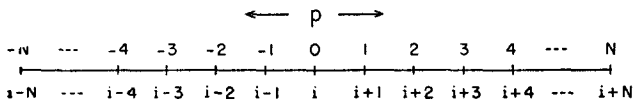

FIG. 1. One-dimensional equally-spaced coordinate.

that equation (7) can be solved as a boundary-value problem if it is of elliptic type. If the absolute vorticity is positive and the ellipticity condition is satisfied, equation (7) reduces to

$$\nabla^2\bar{\Psi} + f = \{2g\nabla^2\bar{z} + f^2 + 4\bar{\Psi}_{xy}{}^2 + (\bar{\Psi}_{xx} - \bar{\Psi}_{yy})^2 - 2\nabla f\cdot\nabla\bar{\Psi}\}^{\frac{1}{2}}. \quad (9)$$

In order to solve (9) for $\bar{\Psi}$ in a given domain, the $\bar{\Psi}$ on the boundary must be prescribed. With the aid of the geostrophic wind relation, the $\bar{\Psi}$ on the boundary may be obtained by integrating the following equation along the boundary (Bolin, 1956),

$$\partial\bar{\Psi}/\partial S = (f^{-1}g)\partial\bar{z}/\partial S - L^{-1}\oint f^{-1}g\delta\bar{z}, \quad (10)$$

where S and L denote a coordinate along the boundary and the total length of the boundary, respectively.

Rewriting (9) in the finite-difference form, the resulting equation is solved for $\bar{\Psi}$ in the grid domain by using a method of the successive approximation which is similar to the one employed by Bushby and Huckle (1956) and Shuman (1957). The details of the present procedure are described elsewhere (Kasahara, 1958).

In order to prevent amplification of high-frequency wave components while solving the vorticity equation, the initial stream-function field was smoothed in such a manner that disturbances of wave length smaller than some critical value l are obliterated, but components of wave length equal to and greater than l are left intact. This smoothing of a two-dimensional field is accomplished by applying a finite-difference smoothing operator discussed by Platzman (1958).

Let $\phi(i)$ denote a function of the one-dimensional equally-spaced discrete coordinate i numbered consecutively (fig. 1). The smoothed function $\tilde{\phi}(i)$ which consists of components of wave length equal to and greater than l is computed from the following formula,

$$\tilde{\phi}(i) = \sum_{p=-N+1}^{N-1}\left[\frac{\sin(2M+1)\xi}{2N\sin\xi}\right]\phi(i+p) + \frac{(-1)^M}{4N}\{\phi(i-N) + \phi(i+N)\}, \quad (11)$$

where $\xi = p\pi/2N$ and $M = 2Nd/l$. Here, p denotes a dummy counter, the origin of which is taken at the point i, as seen in fig. 1. When one constructs the smoothing operator by using $2N+1$ points, placing the center point at the coordinate i, the dummy counter p varies from $-N$ to N. If we denote the distance between two consecutive points by d, the length between the points $i-N$ and $i+N$ becomes $2Nd$. Since l is the critical wave length, the quantity M expresses the corresponding critical wave number. To illustrate, let us take nine points for constructing the operator, so that $N = 4$. Let us choose l as $4d$ so that $M = 2$. Thus, the explicit form of the smoothing formula (11) is shown by

$$\tilde{\phi}(i) = \sum_{p=-4}^{p=4} a_p\phi(i+p), \quad (12)$$

where the numerical values of the a_p's are

$$\begin{aligned} a_0 &= 0.62500, \\ a_1 &= a_{-1} = 0.30178, \\ a_2 &= a_{-2} = -0.12500, \\ a_3 &= a_{-3} = -0.05178, \\ a_4 &= a_{-4} = 0.06250. \end{aligned} \quad (13)$$

It is noted that this smoothing operation does not affect the mean value of a field of infinite extent. In applying the $2N+1$-point formula (11) to a finite set of data, say $\phi_0\cdots\phi_q$, to compute the smoothed field, $\tilde{\phi}_0\cdots\tilde{\phi}_q$, one encounters shortcomings of the data when one performs the operation near the ends of the data set. For example, to obtain $\tilde{\phi}_0$, one must have N additional pieces of data. The method that has been selected to deal with this problem is to assume constant values of ϕ_0 for the additional data. Likewise, we assume a constant value of ϕ_q as the additional data on the other end of the set.

The smoothing operation for a two-dimensional field may be accomplished by successive smoothing in each dimension. First, smooth the data in one dimension with the formula (11) and then smooth the resulting field in the other dimension with the same formula. The initial stream-function field except for the boundary values was smoothed with the formula (12) and the constants (13) and by the process just described, which in effect eliminates the short-wave disturbances of wave length less than four grid intervals.

3. Summary of forecasting results

The periods of hurricanes tested in this experiment are as follows: 11 to 13 (0300 GCT) August 1955 for Connie, 13 to 18 (0300 GCT) August 1955 for Diane, and 13 to 19 (1500 GCT) and 18 to 19 (0300 GCT) August 1956 for Betsy. Both the 500- and 700-mb maps were used for the above periods. The results of the geostrophic (G) and nongeostrophic (NG) forecasts of hurricane movement are presented here, not only to facilitate comparison between the behavior of the two models but also to investigate the forecast errors with a view to further improvement of the prediction models.

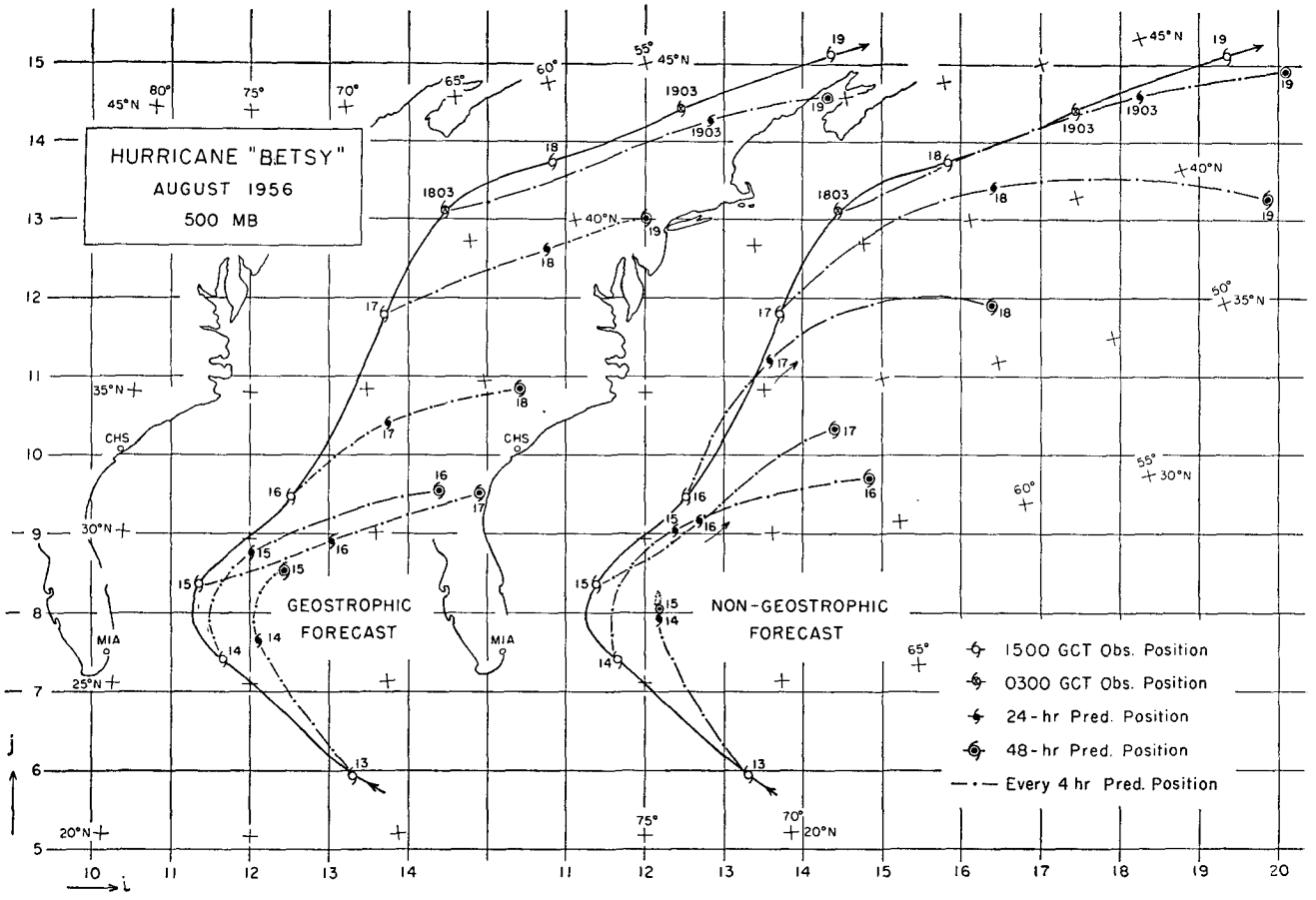

FIG. 2. The 500-mb trajectories of the 24-hr, 48-hr geostrophic and nongeostrophic forecasts and the observed positions of Betsy 13–19 August 1956. Four-hour predicted positions, indicated by dots. Date is identified by numeral beside hurricane symbol.

Let us first consider the sources of forecast errors. In general, errors inherent in the forecast may be classified into the following three types:

1. map analysis errors, especially those due to sparsity of observational data in the tropics;
2. physical modeling errors, due to the assumptions employed for developing a feasible prediction model;
3. mathematical approximation errors, due to the introduction of finite-difference schemes and the specification of boundary conditions.

Since hurricanes appear over ocean areas where upper-air observations generally are sparse, uncertainties in the initial map analysis cause serious difficulties in any attempt to isolate errors of type 1 from those of other types. In the first place, there are some ambiguities in locating the center of the hurricane. Second, because of the fact that the hurricane movement is more or less influenced by the large-scale flow in which it is embedded, the errors of type 1 depend not only upon the accuracy of map analysis over hurricane but also upon large-scale synoptic analysis, such as of subtropical highs and easterly troughs, associated with the hurricane situation. Although it is difficult to assess the magnitude of errors of type 1 in terms of the forecast error of hurricane movement, a rough approximation to the consequences of uncertainties in the initial data is an uncertainty of about 60 n mi in the predicted position of the hurricane.

The reason for using the steering concept in the present models is to reduce large truncation errors (under type 3) which are produced by the presence of the hurricane vortex in the total flow as in ordinary numerical forecasts. The movement of the vortex in the steering flow is, then, predicted with a wind-trajectory computation technique; in addition, the 'vortex interaction' term is included which appears as the second term in (3). Therefore, errors of type 2 arise from the following: first, the shortcoming of the steering-flow forecast with the barotropic model and, second, the insufficient assessment of the 'vortex interaction' in the trajectory calculation. Both sources could give rise to systematic forecast errors.[3] The error due to improper specification of boundary conditions may cause some variations in performance.

The comparisons between the G and NG 24- and 48-hr predicted trajectories of hurricanes Betsy,

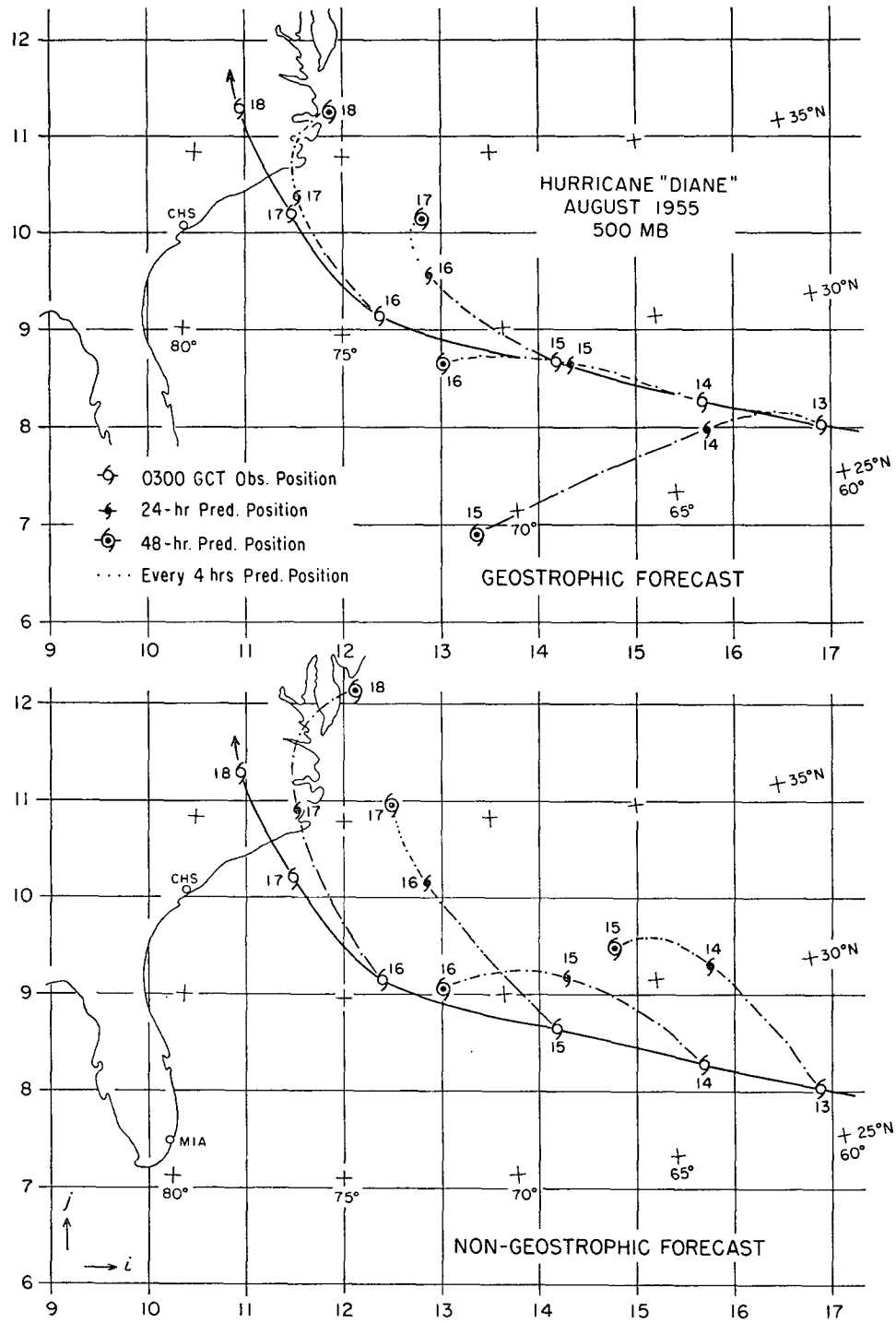

FIG. 3. Same as fig. 2, but for Diane 13–18 August 1955.

[3] The vortex interaction term considered here is derived from the evaluation of the *instantaneous* movement velocity of a barotropic vortex in the large-scale flow. Thus, the physical meaning of the term is essentially analogous to the dynamic term in the well-known Rossby wave formula.

In the hurricane season of 1958, an operational test of hurricane-movement prediction was made using the steering model with the JNWP 500-mb barotropic program. It was found that the over-all influence of the 'vortex interaction' term is beneficial, but that this term contributes to the 24-hr displacement a correction that is less than the uncertainty of the hurricane location (Hubert, 1959). Also, Hubert reported that for five cases the mean trajectory forecast error was 127 n mi, but this figure would be reduced to 57 n mi if the steering flows could be predicted as they were observed. It appears that a large portion of the trajectory forecast error might be due to the shortcoming in the prediction of steering flow.

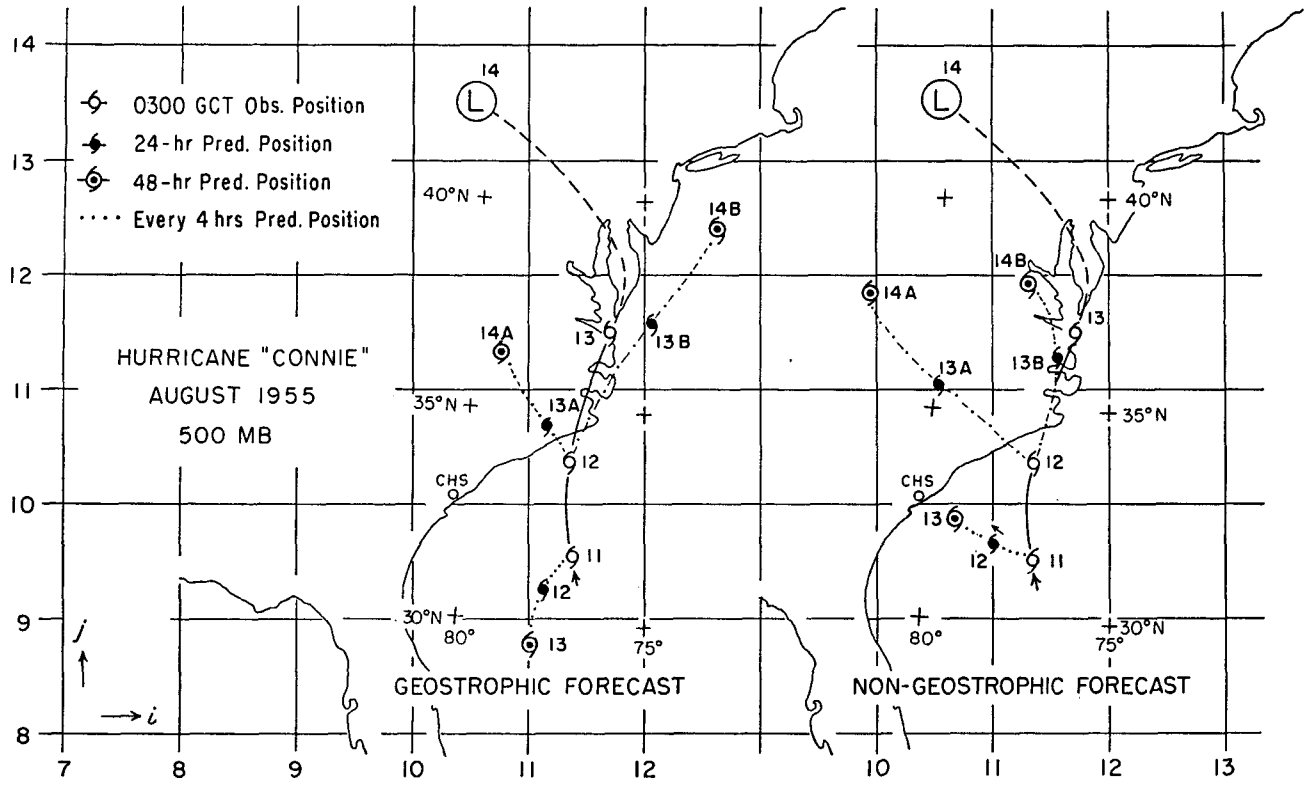

FIG. 4. Same as fig. 2, but for Connie 11–14 August 1955.

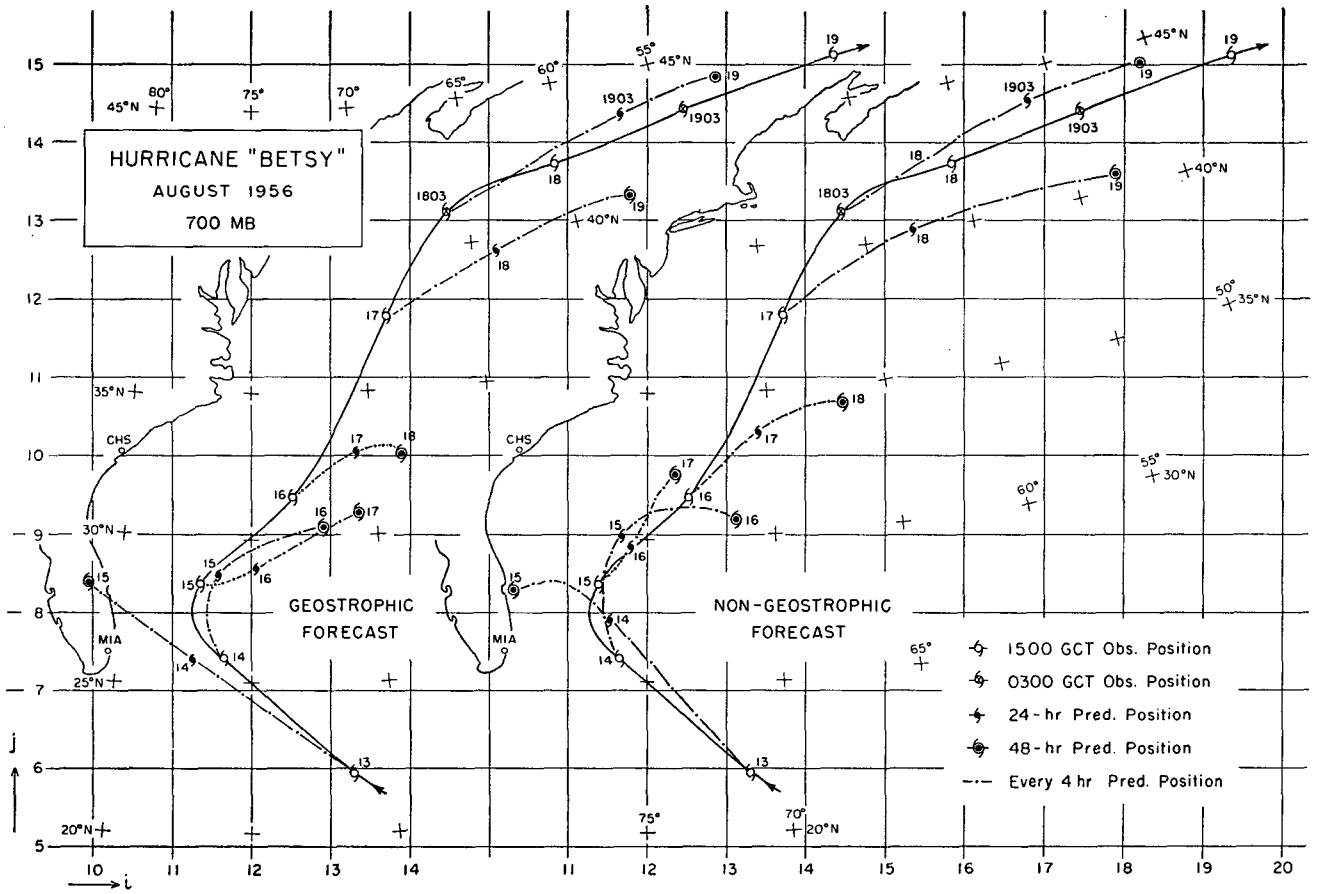

FIG. 5. The 700-mb trajectories of the 24-hr, 48-hr geostrophic and nongeostrophic forecasts and the observed positions of Betsy.

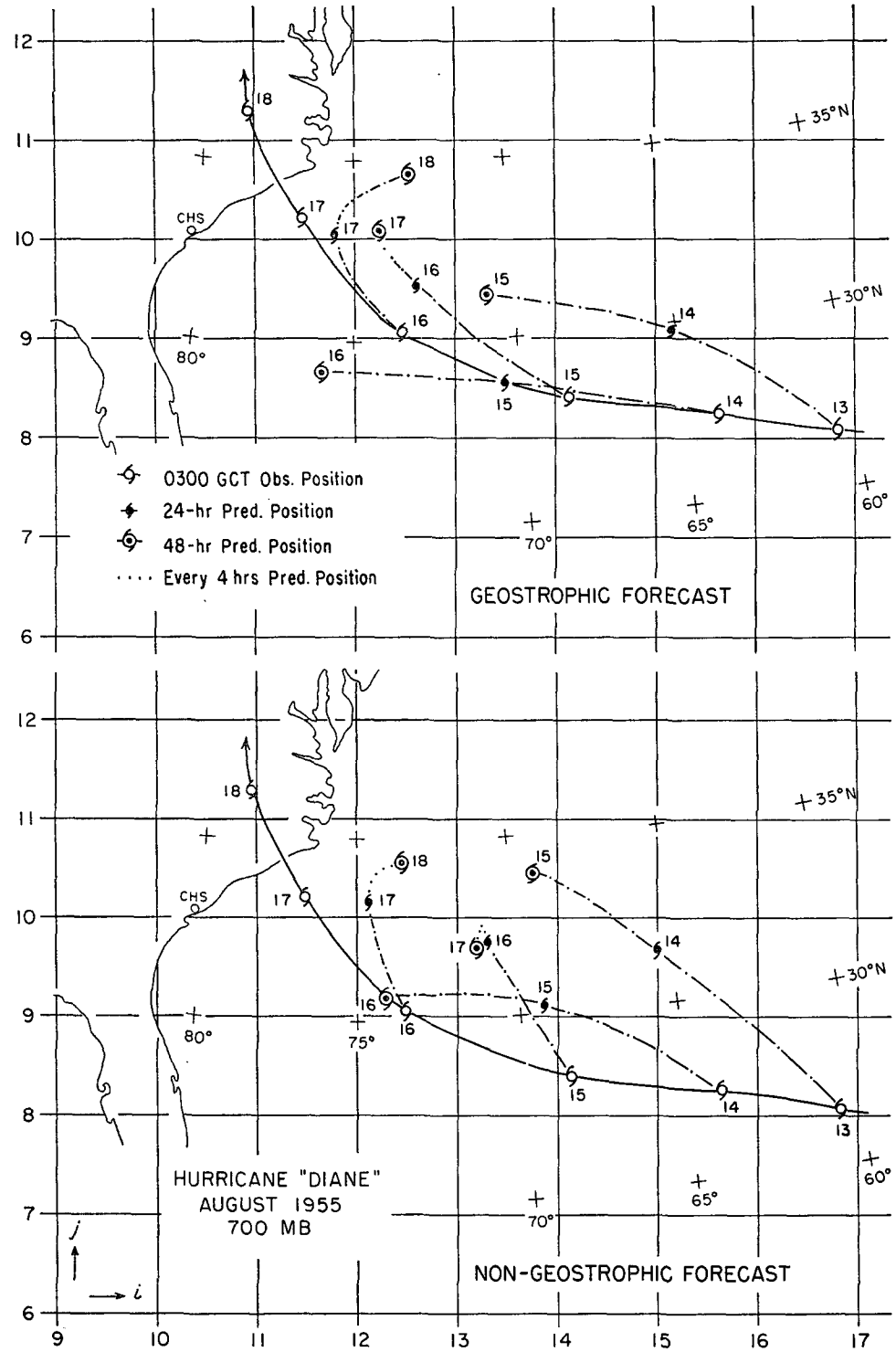

FIG. 6. Same as fig. 5, but for Diane.

Diane, and Connie are illustrated in figs. 2, 3, and 4 for the 500-mb forecasts and in figs. 5, 6, and 7 for the 700-mb forecasts, respectively. The forecast accuracy may be judged by comparing observed and predicted locations of the same date (labeled beside hurricane symbols). The grid mesh in these figures presents one part of the computing network used for predicting the steering flow. The grid distance is 300 km (=162 n mi) at the standard latitudes (30N and 60N). In order to present the results of the G and NG forecasts, the following quantities are considered: the magnitude of the observed displacement vector

TABLE 1. Results of 24-hr forecasts.

Forecast identification	S_{obs}	Geostrophic model S_{pred}	R_s	R_e	E_v	E_s	Nongeostrophic model S_{pred}	R_s	R_e	E_v	E_s
500-mb											
Connie (3)	173	116	0.65	0.84	135	80	129	0.72	0.74	125	44
Diane (4)	244	230	0.95	0.20	51	22	298	1.24	0.57	137	54
Betsy (6)	367	338	0.97	0.41	133	72	403	1.15	0.41	117	69
Total (13)	284	254	0.89	0.45	108	58	308	1.08	0.53	125	58
700-mb											
Connie (2)	168	137	0.83	0.61	95	31	221	1.37	0.78	121	53
Diane (4)	244	291	1.22	0.45	103	76	291	1.25	0.72	165	93
Betsy (6)	367	256	0.73	0.40	149	129	293	0.86	0.43	142	127
Total (12)	293	248	0.91	0.45	124	95	280	1.07	0.58	146	103
Resultant											
Connie (3)	174	123	0 69	0.56	89	51	174	0.99	0 60	100	3
Diane (4)	244	258	1.07	0.23	55	29	294	1.24	0.59	139	51
Betsy (6)	367	296	0.85	0.35	117	85	346	1.00	0.35	102	76
Total (13)	284	244	0.88	0.36	92	60	290	1.07	0.48	112	51

($S_{obs} = |\vec{S}_{obs}|$), the magnitude of the predicted displacement vector ($S_{pred} = |\vec{S}_{pred}|$), the absolute difference between observed and predicted displacements ($E_s = |S_{obs} - S_{pred}|$), the magnitude of the error vector from observed to predicted positions at the end of the forecast period ($E_v = |\vec{S}_{pred} - \vec{S}_{obs}|$), the ratio between predicted and observed displacements ($R_s = S_{pred}/S_{obs}$), and finally the ratio between the magnitude of the error vector and the observed displacement ($R_e = E_v/S_{obs}$). Here, the term 'displacement' is used to refer to the distance between the initial and final points measured in units of one nautical mile. The quantity E_s is determined only by errors in the movement *speed*. On the other hand, E_v is related also to errors in the movement *direction*. In case of the perfect forecast (*i.e.*, $R_e = 0$), E_v should be zero and R_s should be one.

In table 1, there are presented the average values of S_{obs}, S_{pred}, R_s, R_e, E_v, and E_s taken over cases of individual-hurricane- and over 'total'-prediction cases for the 500-mb, 700-mb and 'resultant' 24-hr forecasts. The results of the 'resultant' forecast will be dis-

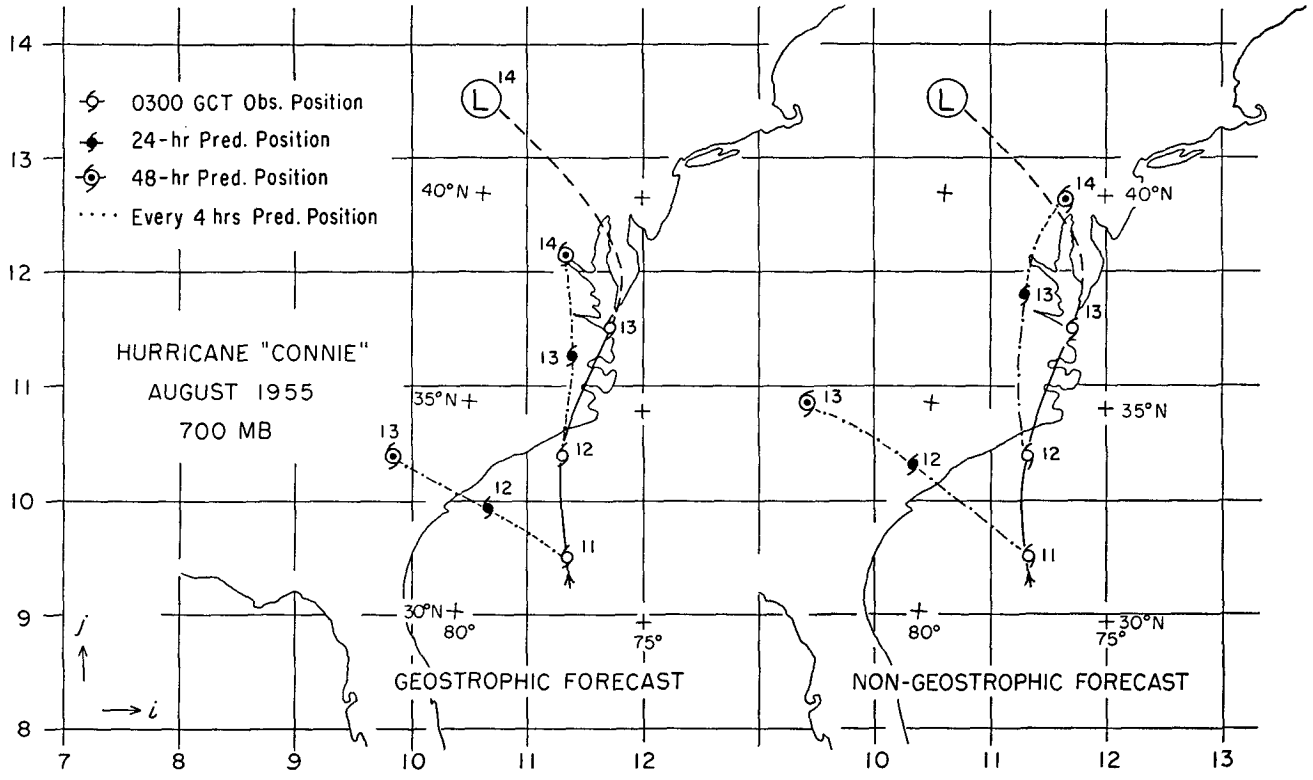

FIG. 7. Same as fig. 5, but for Connie.

TABLE 2. Results of 48-hr forecasts.

Forecast identification	S_{obs}	Geostrophic model S_{pred}	R_s	R_e	E_v	E_s	Nongeostrophic model S_{pred}	R_s	R_e	E_v	E_e
500-mb											
Connie (1)	322	138	0.43	1.42	456	184	128	0.40	0.88	283	194
Diane (4)	481	429	0.91	0.42	200	126	452	0.95	0.39	179	63
Betsy (5)	693	539	0.89	0.56	373	234	677	1.05	0.47	278	126
Total (10)	571	455	0.85	0.59	312	186	532	0.94	0.48	239	108
700-mb											
Connie (1)	329	281	0.85	1.07	351	48	381	1.16	1.17	385	52
Diane (4)	482	481	1.00	0.41	190	146	424	0.89	0.51	234	171
Betsy (5)	693	435	0.73	0.51	380	328	471	0.75	0.44	310	265
Total (10)	572	438	0.85	0.53	301	227	443	0.85	0.54	287	206
Resultant											
Connie (1)	325	152	0.47	1.15	374	173	254	0.78	1.00	325	71
Diane (4)	481	446	0.93	0.32	148	99	438	0.92	0.39	179	83
Betsy (5)	693	481	0.80	0.46	236	261	572	0.89	0.38	247	178
Total (10)	571	434	0.82	0.47	265	188	486	0.89	0.44	227	129

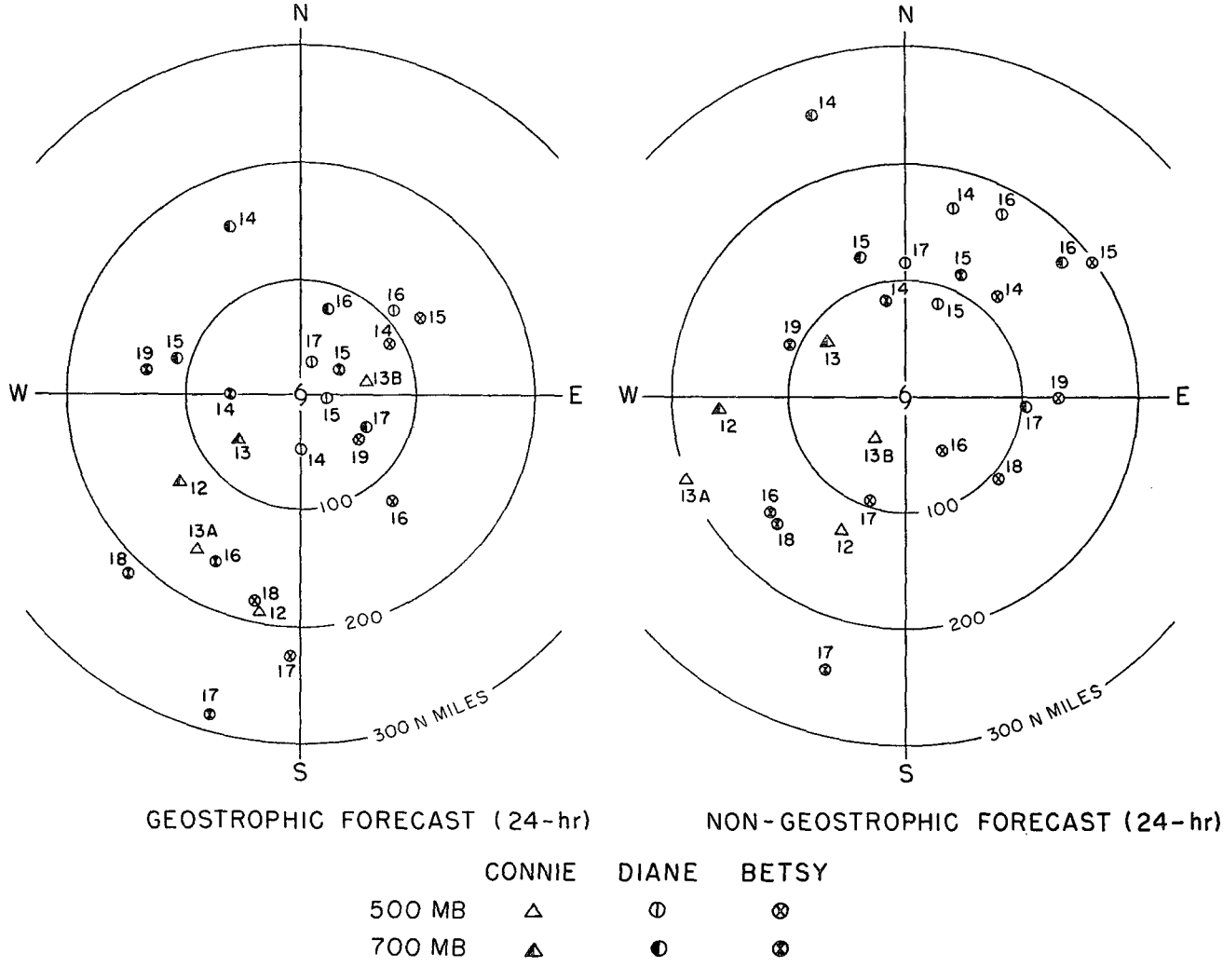

FIG. 8. Polar diagrams of the 500-, 700-mb geostrophic and nongeostrophic 24-hr forecast positions of Betsy, Diane, and Connie relative to the corresponding observed center placed at the center of the diagram. Date valid for each position is indicated by numeral beside each predicted position.

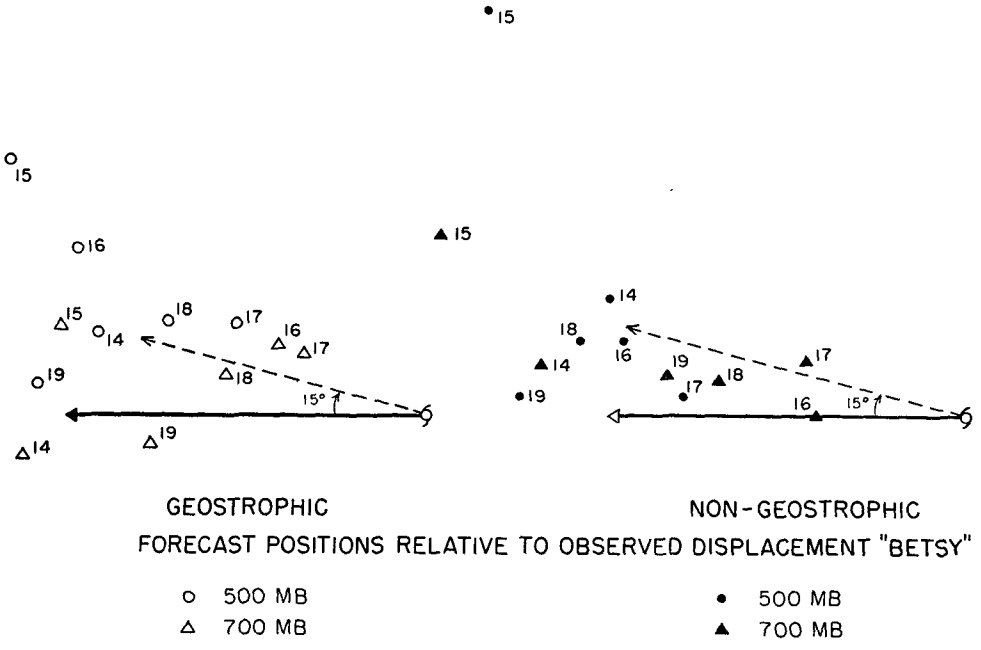

FIG. 9. The 500-, 700-mb geostrophic and nongeostrophic 24-hr forecast positions relative to the observed displacement of Betsy, reducing each observed displacement to the same unit. Date valid for each position as indicated by numeral beside each location.

cussed later. The number of cases used for taking the average of the quantities is denoted inside of the parentheses after each hurricane name. Similar presentations are shown in table 2 for the 48-hr forecasts.

To compare the accuracy of 24-hr NG forecasts with that of G forecasts, fig. 8 is shown. Taking the ordinate towards the north, polar diagrams are constructed with the actual hurricane position at the origin and all 24-hr NG and G forecasts distributed about that center. For the total of 25 cases including 500- and 700-mb 24-hr forecasts, the mean of the magnitude of NG-error vectors is somewhat larger than that of G-error vectors (135 n mi *vs.* 116 n mi). It is seen that forecasts are distributed almost uniformly in each diagram. This implies that the forecast bias relative to geographical direction is not systematic in either NG or G forecasts. However, as is observed from figures 2, 3, 5, and 6, the predicted trajectories display a marked tendency to deflect toward the right of the actual paths. This feature, which is common to Betsy and Diane forecasts, is clearly demonstrated in figs. 9 and 10. Choosing the magnitude of actual 24-hr hurricane displacement as a unit, all 500- and 700-mb 24-hr predicted positions relative to the actual (unit) displacement are plotted in fig. 9 for Betsy and in fig. 10 for Diane. Also shown are the mean relative predicted displacement by a dashed line and the deflection angle of the mean predicted displacement by a number.

A remarkable feature of fig. 10 is the fact that the deflection angle of the NG forecast was even more pronounced than that of the G forecast. Obviously, this is a major cause for deterioration of the NG forecasts of Diane. Another feature observed in the 24-hr NG forecasts of both Diane and Betsy is the increase of predicted displacement compared with the G forecasts. This may be explained from the fact that both hurricanes traveled anticyclonically around the southern periphery of the subtropical high where the nongeostrophic wind speed is generally super-geostrophic.[4]

Concerning the characteristics of Connie forecasts, though the number of cases is insufficient to draw any conclusion, the predicted path shows a tendency of deflecting to the left of the actual path, which is quite the reverse of the results obtained for Diane and Betsy. During the forecast period, Connie moved northwards between the Atlantic subtropical high and a high-pressure cell over the United States. In general, under synoptic situations similar to this, a single-layer barotropic prediction is probably inadequate, simply because the steering current is so weak that those effects which at other times play a minor role in the movement may become the important ones. One such example may be seen from a failure of G

[4] Based upon the wind analyses of the JNWP stream-function fields, it is reported by Carstensen (1958) that the mean magnitude of the stream function (S) winds over the hemisphere is smaller than that of the geostrophic (G) winds. A limit is imposed on the magnitude of the anticyclonic curvature of the stream-function flow (through the ellipticity condition) but not in the cyclonic flow; consequently, the magnitude of the positive values of S-G is limited, whereas the magnitude of the negative values of S-G is not limited. It is conceivable, therefore, that the mean magnitude of the S-winds may become smaller than that of the G-winds if a large random sample is considered.

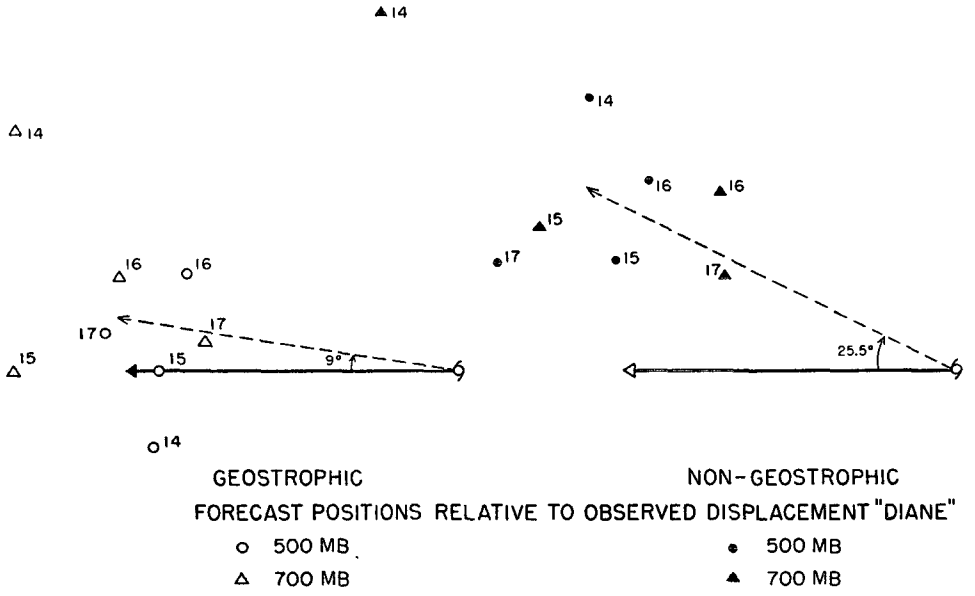

FIG. 10. Same as fig. 9, but for Diane.

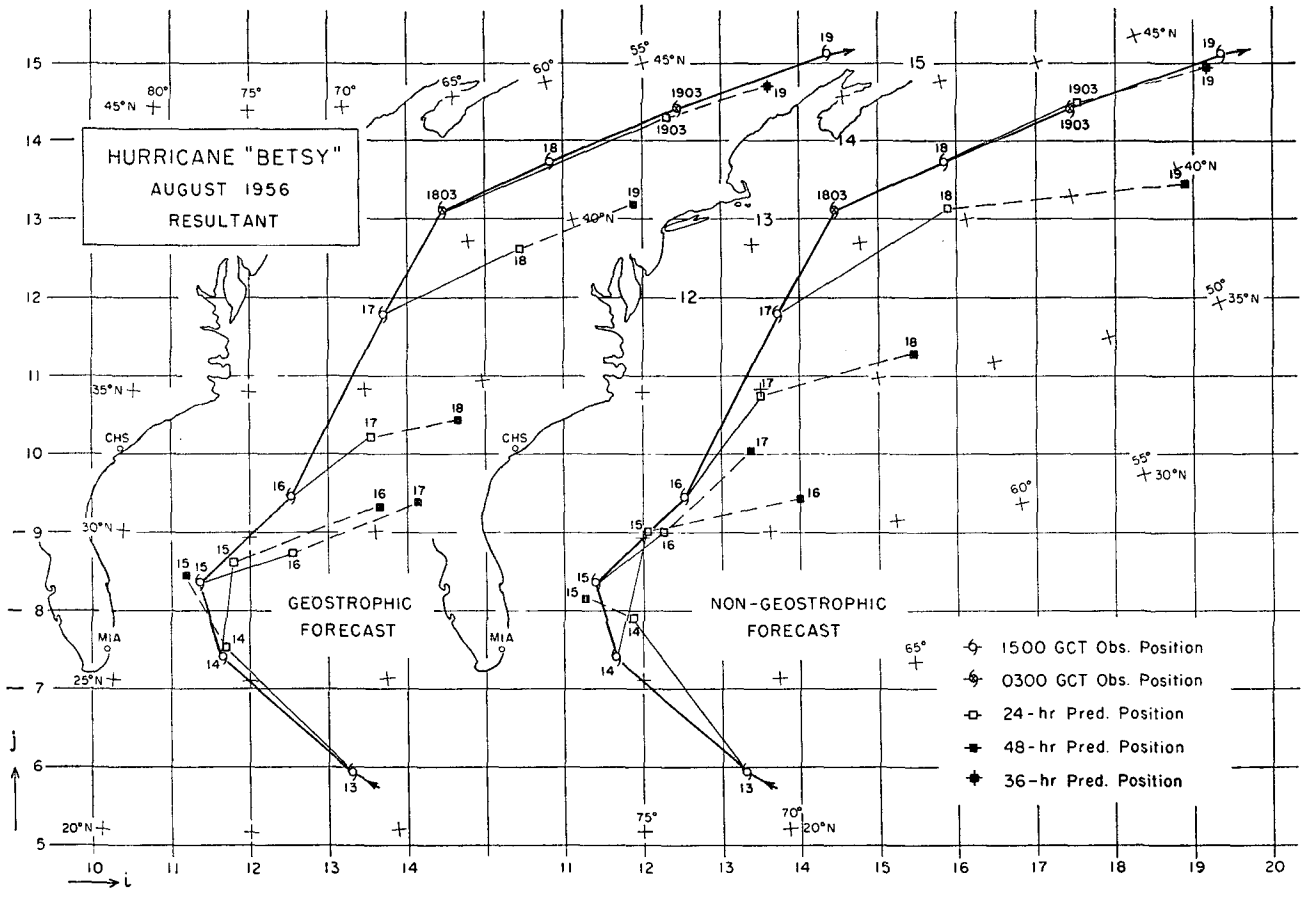

FIG. 11. Trajectories of the 24-hr, 48-hr geostrophic and nongeostrophic 'resultant' forecasts and the observed positions of Betsy.

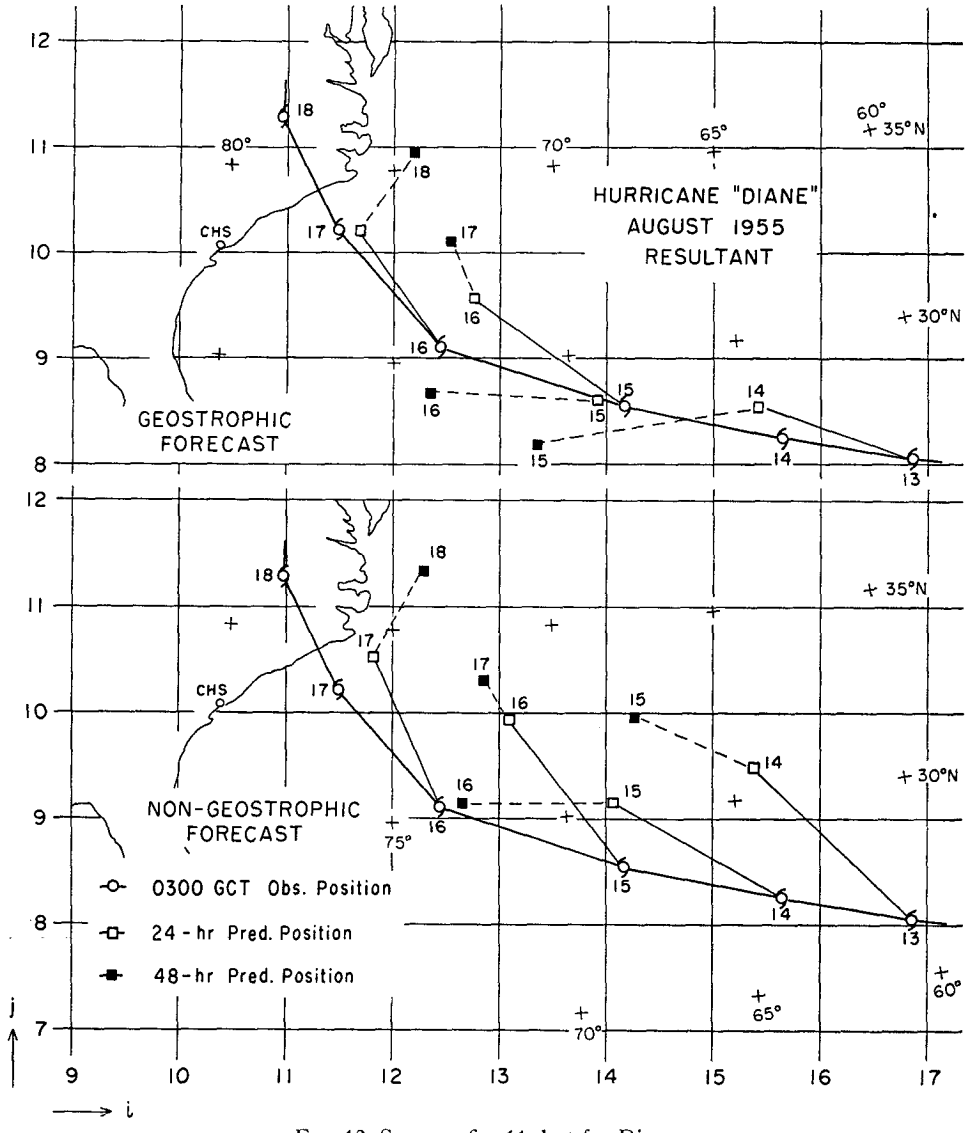

FIG. 12. Same as fig. 11, but for Diane.

forecast beginning with 11 August (see fig. 4). The predicted trajectory runs steadily towards the south instead of moving northwards. On the other hand, the northward component of the movement is predicted by the NG model. This large forecast variation may be explained from the fact that the initial location of the 500-mb Connie was situated near a col (hyperbolic point) of the steering flow; a slight change of the steering flow, due to the process of obtaining the stream function for example, may alter the col position, and the resulting influence may produce gross changes in the movement forecast, although the forecast of the large-scale pattern may be affected only slightly. Also under this circumstance, uncertainties in the initial map analysis are apt to introduce considerable variation in trajectory forecasts. In this connection, we made two independent predictions *A* and *B* based upon two independently analyzed maps *A* and *B* for 0300 GCT 12 August 1955. It is seen from fig. 4 that these two forecasts differ even for the 24-hr period.

On the whole, performances of the two prediction models (NG and G) are essentially comparable, but in some cases both exhibit the same major defect which is a rather consistent forecast bias producing a rightward displacement relative to the actual hurricane path. Since the systematic forecast bias is noticeable even after several hours from the beginning, the effects of the boundary conditions probably do not contribute to this type of error. As stated earlier in this section, it is also unlikely that truncation errors might cause such a bias in the forecasts. In fact, the general characteristics of the Diane and Connie forecasts agree with those obtained independently by Birchfield (1957) with the barotropic geostrophic (150-km grid) prediction model using the same initial maps.

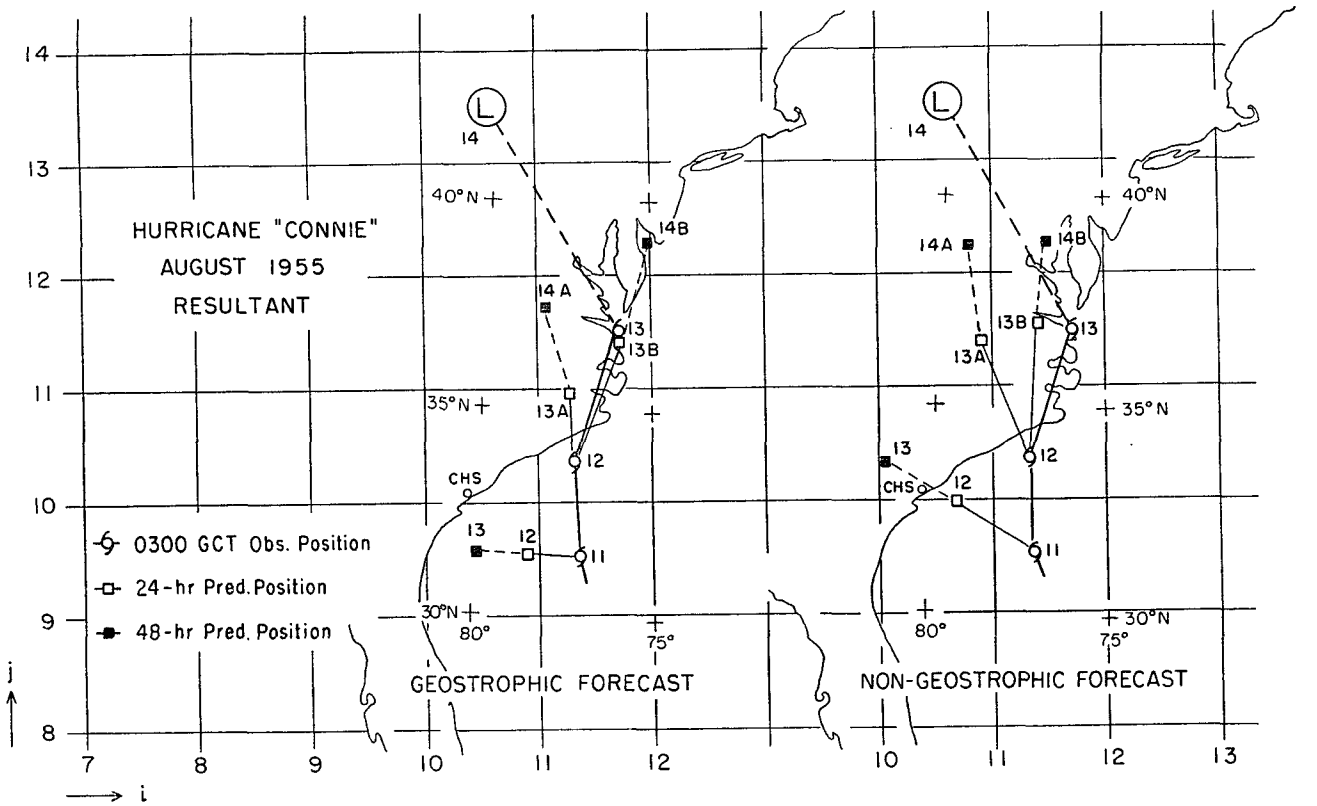

FIG. 13. Same as fig. 11, but for Connie.

The use of the barotropic nondivergent vorticity equation for predicting a large-scale flow is reasonable only when the magnitude of the divergent part of the motion is sufficiently small compared with that of the rotational part. Under this proviso, one may seek the 'nondivergent level' in the atmosphere or one may simulate the 'equivalent nondivergent atmosphere' by computing the vertical average of the motion in the real atmosphere. In the present forecasts, we have regarded the 500-mb or 700-mb surface as the 'nondivergent level.' Therefore, the degree of success in the forecasts depends upon the validity of the nondivergent assumption in the prediction model; hence some systematic variations in performance could be anticipated.

One approach to improve upon the single-layer barotropic predictions may be achieved with the application of the 'equivalent nondivergent' vorticity equation for predicting the evolution of a vertically averaged steering flow. In this model (the mean steering model), the movement of a hurricane may be defined as the movement of the vertically averaged circular vortex. Since we have made two independent sets of barotropic forecasts at the 500- and 700-mb surfaces, the predicted displacement of a vertically averaged vortex at two levels may be obtained by taking the mean of two predicted displacements of 500- and 700-mb hurricanes (Kasahara, 1957b). This is called the 'resultant' predicted displacement. In figs. 11, 12, and 13, the G and NG 24- and 48-hr resultant forecasts of Betsy, Diane, and Connie, respectively, are illustrated. The results of 24- and 48-hr 'resultant' forecasts are presented already in tables 1 and 2. By comparing the magnitudes of average E_v for different cases in these tables, it is seen that the performance of the 'resultant' prediction appears to be the best compared with the results of single-level forecasts. It is conceivable that errors due to motions that do not satisfy the barotropic equations, as well as map analysis errors, could be reduced by averaging two independent forecasts at different levels.

4. Conclusions

The results of this experiment indicate that the numerical methods based on the geostrophic steering model and the nongeostrophic steering model predict the 500-mb or the 700-mb hurricane movement with about equal accuracy. The two trajectory forecasts display a marked similarity and show a tendency to deflect consistently relative to the actual displacements of individual hurricanes. Particularly, in the Diane and Betsy forecasts, the predicted paths lie to the right of the observed tracks. On the other hand, the magnitude of the displacement is generally well predicted.

It seems likely that the systematic errors which we have encountered arise from the shortcomings of the physical model rather than from the mathematical approximations. In other words, as far as the prediction of hurricane is concerned, the *barotropic nondivergent model* itself may contain the major defect no matter how the evaluation of the wind field is improved. Since a tropical cyclone is a huge tropospheric convection cell and the axis of horizontal wind circulation remains almost vertical during the movement, there must be a limit to the simulation of the three-dimensional motion by the two-dimensional barotropic model. To support this point of view, we have shown that the 'resultant' forecast, which is the vector mean of the 700-mb and the 500-mb predicted displacements, yields an encouraging result compared with a single-level barotropic forecast with either the geostrophic model or the nongeostrophic model.

The average forecast error (E_v) between the predicted and observed positions of hurricanes is 110 n mi for the 24-hr period and 230 n mi for the 48-hr period. However, the average error in forecasting the movement speed (E_s) is 50 n mi for the 24-hr period and 130 n mi for the 48-hr period. This suggests that the forecast accuracy will be greatly improved if the movement direction is predicted more accurately.

A program is now being planned to test hurricane forecast with the mean steering model by simulating an 'equivalent barotropic atmosphere' with a vertically averaged steering flow based on 200-, 500-, 700-, and 1000-mb data. By this means, one may hope to reduce systematic forecast errors by suppressing the divergent part of the motion in the atmosphere, which in effect justifies the use of the barotropic nondivergent model. Since the cross-isobaric wind component should deflect the storm to the left of the isobaric flow as it moves around the southern periphery of the subtropical high, the present results indicate that the divergent part of the wind might be responsible to account for the deflection effect observed. In order to explore this possibility as well as the effect of vertical structure of the storm circulation upon the movement, a study is now being undertaken to develop a baroclinic prediction model; this will be the subject of a later report.

Acknowledgments.—The writer would like to express his sincere gratitude to Professor George W. Platzman for his helpful comments in the preparation of this article. The writer would also like to extend acknowledgments to Professor Herbert Riehl for his valuable advice on the initial map analysis, and to Mr. Robert H. Simpson, Director of the National Hurricane Research Project, for arranging to send us necessary data materials for analysis of hurricane Betsy. Thanks are also due to Mr. Gene E. Birchfield for helpful discussions.

The numerical computations were performed by the IBM-704 electronic computer at the U. S. Weather Bureau, Suitland, Maryland. In this connection, the writer is indebted to Dr. Joseph Smagorinsky, Director of the General Circulation Research Section, and his associates for facilitating our use of the computer.

REFERENCES

Birchfield, G. E., 1957: *Numerical prediction of hurricane movement with the use of a fine grid.* Dept. Meteor., Univ. Chicago, 15 pp.

Bolin, B., 1955: Numerical forecasting with the barotropic model. *Tellus*, **7**, 27–49.

——, 1956: An improved barotropic model and some aspects of using the balance equation for three-dimensional flow. *Tellus*, **8**, 61–75.

Bushby, F. H., and V. M. Huckle, 1956: The use of a stream function in a two-parameter model of the atmosphere. *Quart. J. r. meteor. Soc.*, **82**, 409–418.

Carstensen, L. P., 1958: *The comparison of geostrophic and stream winds with observed winds.* Tech. Mem. 14, Joint Numer. Wea. Predic. Unit, Washington, D. C.

Charney, J., 1955: The use of the primitive equations of motion in numerical prediction. *Tellus*, **7**, 22–26.

Hubert, L. F., 1959: *A test of numerical hurricane prediction under operational conditions.* Dept. Meteor., Univ. Chicago, 31 pp.

Hubert, W. E., 1957: Hurricane trajectory forecasts from a nondivergent, non-geostrophic, barotropic model. *Mon. Wea. Rev.*, **85**, 83–87.

Kasahara, A., 1957a: The numerical prediction of hurricane movement with the barotropic model. *J. Meteor.*, **14**, 386–402.

——, 1957b: *A test of the barotropic numerical prediction of hurricane movement at the 700-mb level.* Dept. of Meteor., Univ. Chicago, 21 pp.

——, 1958: *A comparison between geostrophic and non-geostrophic numerical forecasts of hurricane movement with the barotropic steering model.* Dept. Meteor., Univ. Chicago, 46 pp.

Masuda, Y., and H. Itoo, 1957: The use of a stream function for the barotropic forecast of the typhoon movement. *J. meteor. Soc. Jap.*, 75th Anniversary Vol., 296–303.

Palmén, E., and H. Riehl, 1957: Budget of angular momentum and energy in tropical cyclones. *J. Meteor.*, **14**, 150–159.

Platzman, G. W., 1958: *An approximation to the product of discrete functions.* Dept. Meteor., Univ. Chicago, 23 pp.

Shuman, F. G., 1957: Numerical methods in weather prediction: I. The balance equation. *Mon. Wea. Rev.*, **85**, 329–332.